Supplementary information for 'Magnetic oscillations induced by phonons in non-magnetic materials'

Supplementary Figures

In Figures. 1 and 2 of the main text we show the induced magnetization in real space for an in-plane and an out-of-plane displacement of the W atoms, respectively. In this section we show supplementary figures to those presented in the main text. In particular, supplementary Figs. 1 and 2 display the induced magnetization in real space for an in-plane and an out-of-plane displacement of the W atoms for $\mathbf{q} = \mathbf{K}' = -\mathbf{K}$, respectively, while supplementary Figs. 3 and 4 do the same for $\mathbf{q} = \mathbf{M}$. All the figures shown in the main text and in the supplementary material are snapshots of the time evolution of the induced magnetization for each mode. This time evolution can be seen in the Supplementary Movies.

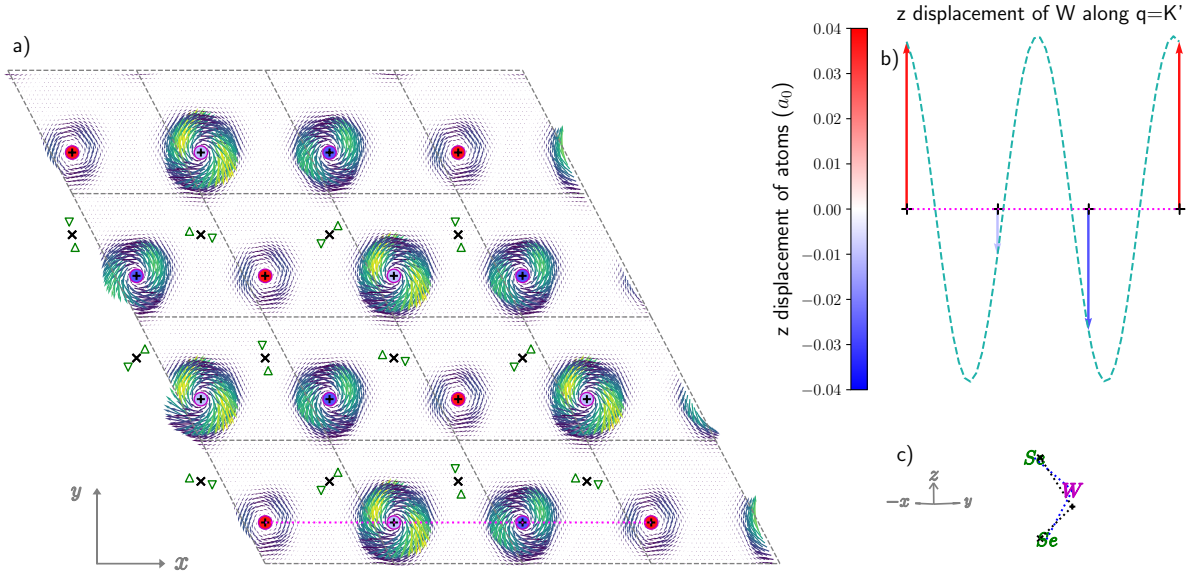

Supplementary Figure 1: **Real-space representation of the induced magnetization for the second lowest energy acoustic phonon mode at $\mathbf{q} = \mathbf{K}' = -\mathbf{K}$ involving pure out-of-plane displacements of W atoms.** This is the time-reversed image of Fig. 1 of the main text. **a)** Magnetization in the W plane showing 4×4 unit cells along the hexagonal axes of WSe_2 for the the second lowest energy mode at $\mathbf{q} = \mathbf{K}' = -\mathbf{K}$ (in orange in Figs. 3**a** and 3**b** of the main text). In this mode the W atoms (filled circles) displace along the perpendicular direction (see colour-bar) and Se atoms above (filled triangle up) and below (filled triangle down) the W plane rotate anticlockwise with opposite phase around their equilibrium positions (crosses) in their respective planes. The coloured vector-field is proportional to the in-plane magnetization at each point in real space, with yellow/light (blue/dark) arrows representing the largest (smallest) values. These arrows as well as the displacements of the Se atoms have been scaled to make them visible. **b)** The coloured arrows give the z displacement of the W atoms along the $\mathbf{q} = \mathbf{K}'$ direction (dotted magenta line in panel **a)**) according to the same colour-bar. The dashed line describes the propagation of the vibration along several unit-cells in real space. Note that $\mathbf{K}' = [2/3, -1/3, 0] = -\mathbf{K}$ in crystal axes and therefore it shows the same propagation as in Fig. 1**b** of the main text but looked from right to left. **c)** Side view of the WSe_2 formula-unit in the lower left corner unit-cell. The names of the atoms display their displacements from the equilibrium positions, denoted as in panel **a)**. This figure is a snapshot of the time evolution of the induced magnetization for this mode (Supplementary Movie 3).

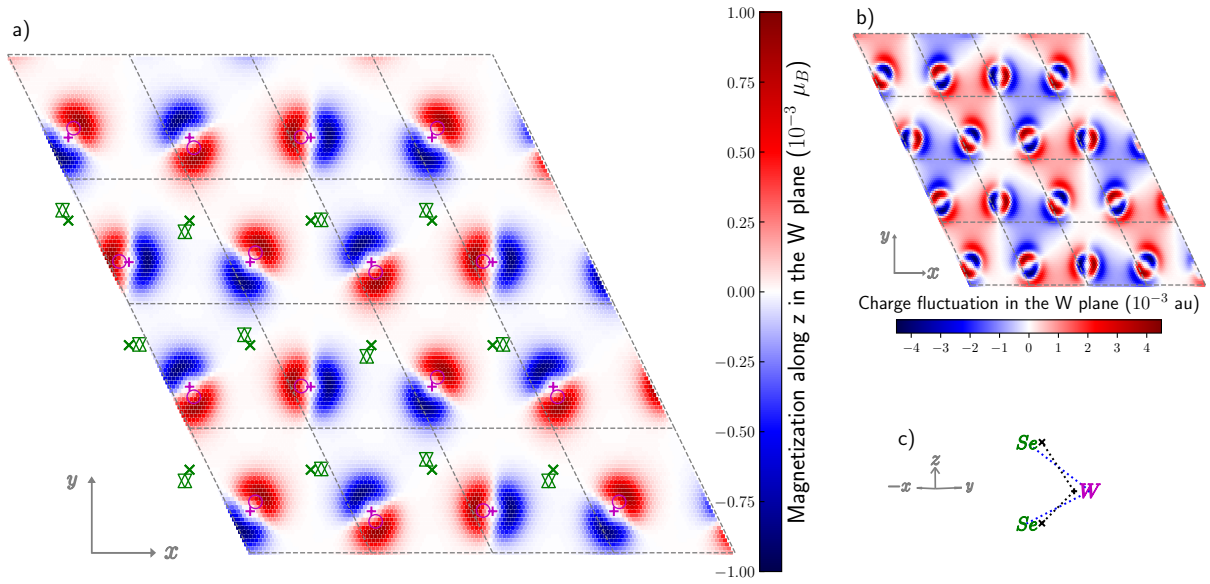

Supplementary Figure 2: **Real-space representation of the induced magnetization for the highest energy acoustic phonon mode at $\mathrm{q} = \mathrm{K}' = -\mathrm{K}$ involving in-plane displacements of the W atoms.** This is the time-reversed image of Fig. 2 of the main text. **a)** Perpendicular component of the magnetization in 4×4 unit cells along the hexagonal axes of WSe_2 for the third lowest phonon mode for $\mathbf{q} = \mathbf{K}' = -\mathbf{K}$ (represented in green in Figs. 3**a** and 3**c**. This mode is composed by anticlockwise rotations of the W atom (circles) around its equilibrium position and in-phase clockwise rotations of the Se atoms located above (triangle up) and below (triangle down) the W plane. The colour code shows the magnetization in the perpendicular direction. The displacements of the atoms have been scaled to make them visible. **b)** Induced electronic charge for the same atomic configuration as in panel **a)**. **c)** Side view of the WSe_2 formula-unit in the lower left corner unit-cell. The names of the atoms display their displacements from the equilibrium positions, denoted as in panel **a)**. This figure is a snapshot of the time evolution of the magnetic fluctuations for this mode (Supplementary Movie 4).

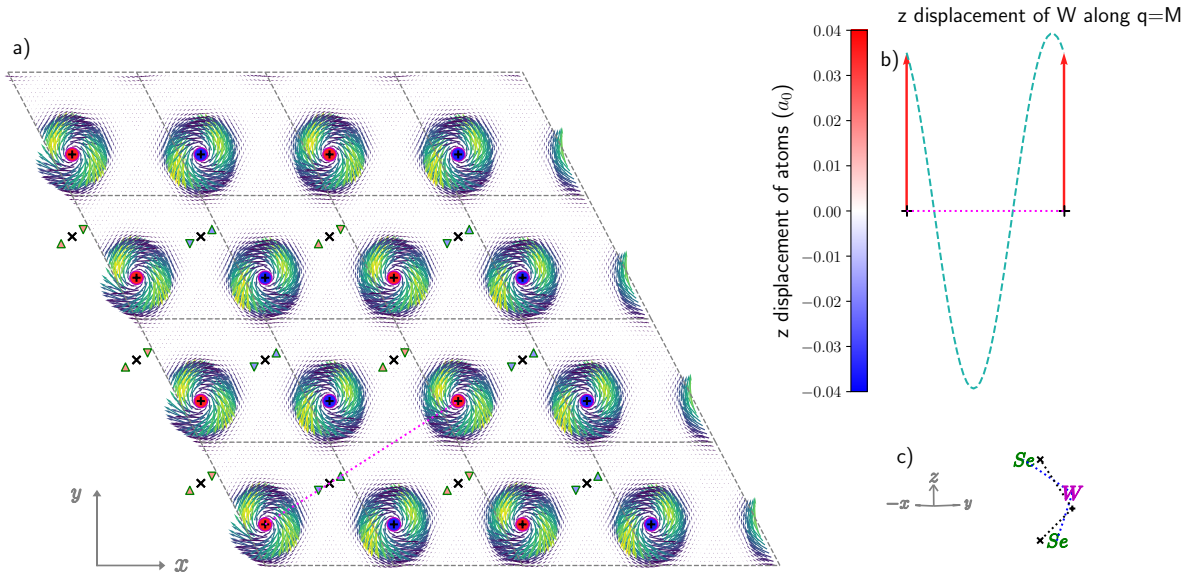

Supplementary Figure 3: **Real-space representation of the induced magnetization for the second lowest energy acoustic phonon mode at $\mathbf{q} = \mathrm{M}$ involving pure out-of-plane displacements of W atoms. a)** Magnetization in the plane of the W atoms for 4×4 unit cells along the hexagonal axes of WSe_2 for the second lowest energy mode at $\mathbf{q} = \mathrm{M}$ (in orange in Figs. 3**a** and 3**b**). In this mode the W atoms (filled circles) displace along the perpendicular direction to the plane while Se atoms above (filled triangle up) and below (filled triangle down) the W plane move linearly along $\mathbf{q} = \mathrm{M}$ around their equilibrium positions (crosses) in their respective planes. The coloured vector-field is proportional to the in-plane magnetization at each point in real space, with yellow/light (blue/dark) arrows representing the largest (smallest) values. These arrows as well as the displacements of the Se atoms have been scaled to make them visible. **b)** The coloured arrows give the z displacement of the W atoms along the $\mathbf{q} = \mathrm{M}$ direction (dotted magenta line in panel **a)**) according to the same colour-bar. The dashed line describes the propagation of the vibration along several unit-cells in real space. Note that $\mathrm{M} = [1/2, 0, 0]$ in crystal axes, and hence the periodicity of the wave. **c)** Side view of the WSe_2 formula-unit in the lower left corner unit-cell. The names of the atoms display their displacements from the equilibrium positions, denoted as in panel **a)**. This figure is a snapshot of the time evolution of the magnetization for this mode (Supplementary Movie 5).

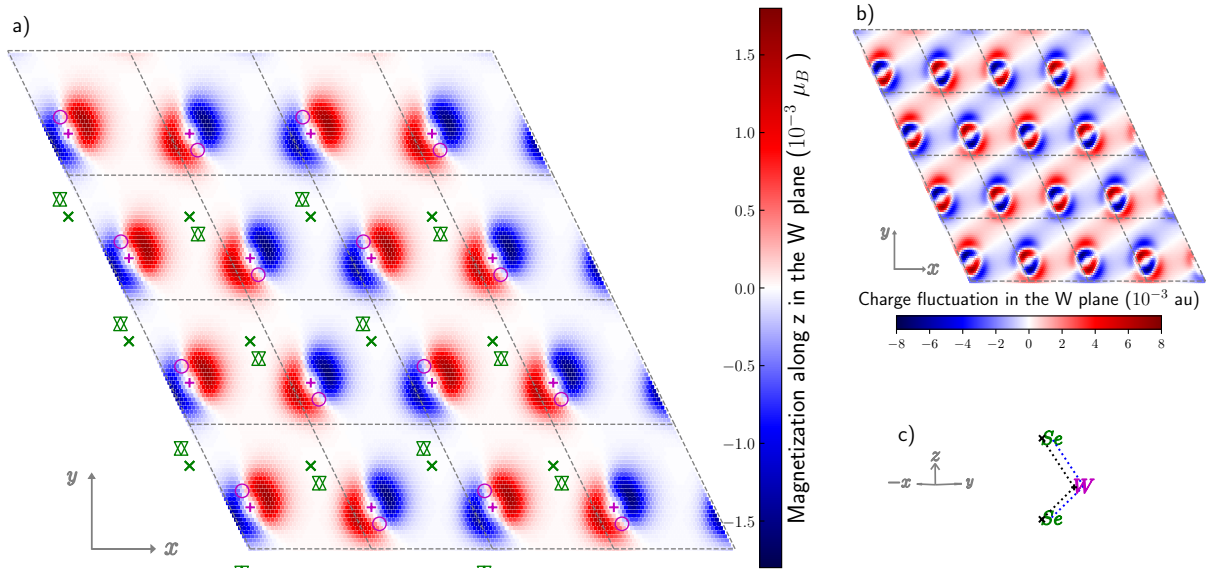

Supplementary Figure 4: **Real-space representation of the induced magnetization for the lowest energy acoustic phonon mode at** $\mathrm{q} = \mathrm{M}$ **involving in-plane displacements of the W atoms. a)** Perpendicular component of the magnetization in 4×4 unit cells along the hexagonal axes of WSe_2 for the lowest phonon mode for $\mathbf{q} = \mathrm{M}$ (represented in blue in Figs. 3**a** and 3**c**). In this mode all atoms displace linearly in the plane at right angles with the direction of the phonon propagation $\mathbf{q} = \mathrm{M}$. The colour code represents the magnetization in the perpendicular direction. The displacements of the atoms have been scaled to make them visible. **b)** Induced electronic charge for the same atomic configuration as in panel **a)**. **c)** Side view of the WSe_2 formula-unit in the lower left corner unit-cell. The names of the atoms display their displacements from the equilibrium positions, denoted as in panel **a)**. This figure is a snapshot of the time evolution of the induced magnetization for this mode (Supplementary Movie 6).

Supplementary Note 1: *Ab initio* calculations

The first-principles calculations were performed within the non-collinear density functional theory (DFT) [1, 2] and density functional perturbation theory (DFPT) [3, 4] using fully relativistic norm-conserving pseudopotentials as implemented in the QUANTUM ESPRESSO (QE) package [5]. For a given displacement pattern α and wave vector $\mathbf{q}$, QE solves the Sternheimer equation in the non-collinear regime [4],

$$\left(H^{\sigma,\sigma'}(\mathbf{r}) - \epsilon_{\mathbf{k},i}\right) \delta^{\mathbf{q},\alpha}\Psi^{\sigma'}_{\mathbf{k},i}(\mathbf{r}) + \delta H^{\sigma,\sigma'}_{\mathbf{q},\alpha}(\mathbf{r})\ \Psi^{\sigma'}_{\mathbf{k},i}(\mathbf{r}) = 0 \tag{1}$$

self-consistently for the first order variation of the electron spinor wave functions $\delta^{\mathbf{q},\alpha}\Psi^{\sigma'}_{\mathbf{k},i}(\mathbf{r})$ and the variation of the potential $\delta H^{\sigma,\sigma'}_{\mathbf{q},\alpha}$ [3]. Above $\Psi^{\sigma}_{\mathbf{k},i}$ and $\epsilon_{\mathbf{k},i}$ denote the unperturbed Kohn-Sham spinor wave functions and energies, $H^{\sigma,\sigma'}\Psi^{\sigma'}_{\mathbf{k},i} = \epsilon_{\mathbf{k},i}\Psi^{\sigma}_{\mathbf{k},i}$. The induced (frozen) spin-charge density matrix is given by

$$\delta n^{\sigma,\sigma'}_{\mathbf{q},\alpha}(\mathbf{r}) = 2\ \mathrm{Re}\left(\sum_{\mathbf{k},i}^{\mathrm{occ}} \langle \Psi^{\sigma'}_{\mathbf{k},i}(\mathbf{r})\, |\delta^{\mathbf{q},\alpha}\Psi^{\sigma'}_{\mathbf{k},i}(\mathbf{r})\rangle\right). \tag{2}$$

However, keeping the complex wave character

$$\sum_{\mathbf{k},i}^{\mathrm{occ}} \langle \Psi^{\sigma'}_{\mathbf{k},i}(\mathbf{r})\, |\delta^{\mathbf{q},\alpha}\Psi^{\sigma'}_{\mathbf{k},i}(\mathbf{r})\rangle = \sum_{\mathbf{k},i}^{\mathrm{occ}} \langle u^{\sigma'}_{\mathbf{k},i}(\mathbf{r})\, |\delta^{\mathbf{q},\alpha}u^{\sigma'}_{\mathbf{k},i}(\mathbf{r})\rangle\, e^{i\mathbf{qr}} = \delta\tilde{n}^{\sigma,\sigma'}_{\mathbf{q},\nu}(\mathbf{r})e^{i\mathbf{qr}}, \tag{3}$$

where $\delta\tilde{n}^{\sigma,\sigma'}_{\mathbf{q},\nu}(\mathbf{r})$ is the periodic part of the complex spin-charge density matrix, and for a spatial translation by a lattice vector $\mathbf{R}$, $\delta\tilde{n}^{\sigma,\sigma'}_{\mathbf{q},\nu}(\mathbf{r}-\mathbf{R}) = \delta\tilde{n}^{\sigma,\sigma'}_{\mathbf{q},\nu}(\mathbf{r})$.

Even though WSe_2 is obviously a non-magnetic material, we considered the magnetic calculation (broken time reversal) within the QE package. The ground state was calculated considering the non-collinear and magnetic case, and obviously, the system converged into a state with null overall magnetization. This procedure allowed us to consider the Sternheimer equation in the most general case and including the four components of the generalized induced charge/potential as described in the main text.

The ground-state electronic and phonon structures of the single-layer WSe_2 were obtained with a hexagonal cell parameter $a = 6.12\ a_0$ and a vacuum layer of 4 times the lattice parameter, which is large enough for avoiding any interplay between adjacent layers. All atomic forces were relaxed up to at least 10^{-7} Rya_0^{-1} . We used a 16×16 Monkhorst-Pack grid for the self-consistent electronic calculations, while the lattice vibrational properties were evaluated on a coarse 8×8 q-point mesh. Convergence was checked by doubling the latter.

Supplementary Note 2: Relation between the magnetic fluctuation and the dynamic structure factor

In this section we derive the relation between equation (3) of the main text and the dynamic structure factor.

Let $\delta\tilde{M}^{\alpha}_{\mathbf{q},\nu}(\mathbf{r})$ denote the periodic part of the magnetic components of the frozen charge-spin density wave for the phonon mode ν with momentum $\mathbf{q}$ in the cartesian direction α, as described in equation (2) of the main text. The fluctuation of the unit-cell average of the time-dependent spin-field is proportional to

$$\overline{\delta M^{\alpha}_{\mathbf{q},\nu}} = \sqrt{\left\langle \left(\mathrm{Re} \int_{\Omega} \frac{d^3\mathbf{r}}{\Omega} \delta\tilde{M}^{\alpha}_{\mathbf{q},\nu}(\mathbf{r}) e^{-i\omega_{\mathbf{q},\nu}t} \right)^2 \right\rangle_T - \left(\left\langle \mathrm{Re} \int_{\Omega} \frac{d^3\mathbf{r}}{\Omega} \delta\tilde{M}^{\alpha}_{\mathbf{q},\nu}(\mathbf{r}) e^{-i\omega_{\mathbf{q},\nu}t} \right\rangle_T \right)^2} \quad (4)$$

Using for the unit-cell average $\delta\bar{m}^{\alpha}_{\mathbf{q},\nu} = \int_{\Omega} \frac{d^3\mathbf{r}}{\Omega} \delta\tilde{M}^{\alpha}_{\mathbf{q},\nu}(\mathbf{r})$, then

$$\begin{aligned} \mathrm{Re}\left(\int_{\Omega} \frac{d^3\mathbf{r}}{\Omega} \delta\tilde{M}^{\alpha}_{\mathbf{q},\nu}(\mathbf{r}) e^{-i\omega_{\mathbf{q},\nu}t} \right) &= \mathrm{Re}\left(\delta\bar{m}^{\alpha}_{\mathbf{q},\nu} e^{-i\omega_{\mathbf{q},\nu}t} \right) \\ &= \mathrm{Re}\left(\delta\bar{m}^{\alpha}_{\mathbf{q},\nu} \right) \cos(\omega_{\mathbf{q},\nu}t) + \mathrm{Im}\left(\delta\bar{m}^{\alpha}_{\mathbf{q},\nu} \right) \sin(\omega_{\mathbf{q},\nu}t). \end{aligned} \quad (5)$$

Since the time average of the trigonometric functions is null, $\langle \cos(\omega_{\mathbf{q},\nu}t) \rangle_T = \langle \sin(\omega_{\mathbf{q},\nu}t) \rangle_T = 0$, the second term in the right-hand side in equation (4) vanishes and we obtain equation (3) of the main text. Replacing equation (5) and using $\langle \cos^2(\omega_{\mathbf{q},\nu}t) \rangle_T = \langle \sin^2(\omega_{\mathbf{q},\nu}t) \rangle_T = \frac{1}{2}$

$$\begin{aligned} \left(\overline{\delta M^{\alpha}_{\mathbf{q},\nu}} \right)^2 \sim \left\langle \left(\mathrm{Re} \int_{\Omega} \frac{d^3\mathbf{r}}{\Omega} \delta\tilde{M}^{\alpha}_{\mathbf{q},\nu}(\mathbf{r}) e^{-i\omega_{\mathbf{q},\nu}t} \right)^2 \right\rangle_T &= \frac{1}{2} \left[\left(\mathrm{Re}\left(\delta\bar{m}^{\alpha}_{\mathbf{q},\nu} \right) \right)^2 + \left(\mathrm{Im}\left(\delta\bar{m}^{\alpha}_{\mathbf{q},\nu} \right) \right)^2 \right] \\ &= \frac{1}{2} |\delta\bar{m}^{\alpha}_{\mathbf{q},\nu}|^2. \end{aligned} \quad (6)$$

Therefore it is proved that the square of the magnetic fluctuation is proportional to the absolute value of the unit-cell average of the magnetisation in each cartesian direction α, which is, in turn, proportional to the diagonal spectral contribution to equation (5) in the main text.

Supplementary References

[1] Hohenberg, P. & Kohn, W. Inhomogeneous electron gas. *Phys. Rev.* **136**, B864–B871 (1964).

[2] Kohn, W. & Sham, L. J. Self-consistent equations including exchange and correlation effects. *Phys. Rev.* **140**, A1133–A1138 (1965).

[3] Baroni, S., de Gironcoli, S., Dal Corso, A. & Giannozzi, P. Phonons and related crystal properties from density-functional perturbation theory. *Rev. Mod. Phys.* **73**, 515–562 (2001).

[4] Dal Corso, A. Density functional perturbation theory for lattice dynamics with fully relativistic ultrasoft pseudopotentials: Application to fcc-pt and fcc-au. *Phys. Rev. B* **76**, 054308 (2007).

[5] Giannozzi, P. *et al.* Quantum espresso: a modular and open-source software project for quantum simulations of materials. *Journal of Physics: Condensed Matter* **21**, 395502 (2009).